# Galaxy Clusters

Emily Safsten and Malinda Baer

# Cluster counts as tracers of dark energy

Expected number of halos in mass bin *a* and redshift bin *i* in solid angle ΔΩ:

$$\overline{N}(M_a, z_i) \equiv \overline{N}_{ai} = \frac{\Delta\Omega_i}{4\pi} \int_{z_i}^{z_{i+1}} dz \, \frac{dV}{dz} \int_{\ln M_a}^{\ln M_{a+1}} d \, \ln M \, \frac{dn}{d \, \ln M}$$

- Contains both expansion history (volume element) and matter density (mass function)

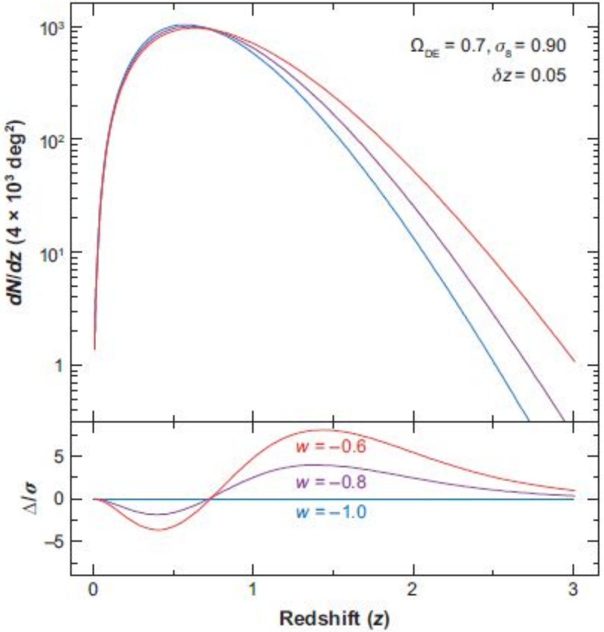


**Figure 13**

Predicted cluster counts for a survey covering 4000 deg², which is sensitive to halos more massive than $2 \times 10^{14}$ $M_\odot$, for three flat cosmological models with fixed $\Omega_M = 0.3$ and $\sigma_8 = 0.9$. *Bottom*: Differences between the models relative to the statistical errors. Reproduced from Mohr (2005).

Figure from Frieman et al. (2008)

# Other dark energy tracers

- Distance measures:

  - Hot gas fraction $f(z) \propto d(z)^{3/2}$ because, as measured from X-ray observations, gas mass $\propto d^{5/2}$ but total mass $\propto d$
  - Combination of Sunyaev-Zel'dovich and X-ray observations, based on an observed SZ signal and a predicted signal based on X-ray observations, which depend on distance, of the intracluster medium

- Power spectrum of angular SZ distortions of CMB -- contains expansion history and matter density

# Current efforts and recent results

**Table 2 Recent cosmological results from galaxy clusters[a,b]**

| Reference[c] | Data | $\sigma_8$ | $\Omega_m$ | $\Omega_{DE}$ | $w$ | $b$ |
|---|---|---|---|---|---|---|
| **Local abundance and evolution[d]** | | | | | | |
| M10 | X-ray | $0.82 \pm 0.05$ | $0.23 \pm 0.04$ | $1 - \Omega_m$ | $-1.01 \pm 0.20$ | |
| V09 | X-ray | $0.81 \pm 0.04$ | $0.26 \pm 0.08$ | $1 - \Omega_m$ | $-1.14 \pm 0.21$ | |
| **Local abundance only** | | | | | | |
| R10 | optical | $0.80 \pm 0.07$ | $0.28 \pm 0.07$ | $1 - \Omega_m$ | $-1$ | |
| H09 | X-ray | $0.88 \pm 0.04$ | 0.3 | $1 - \Omega_m$ | $-1$ | |
| **Local abundance and clustering** | | | | | | |
| S03 | X-ray | $0.71^{+0.13}_{-0.16}$ | $0.34^{+0.09}_{-0.08}$ | $1 - \Omega_m$ | $-1$ | |
| **Gas-mass fraction** | | | | | | |
| A08 | X-ray | | $0.27 \pm 0.06$ | $0.86 \pm 0.19$ | $-1$ | |
| A08 | X-ray | | $0.28 \pm 0.06$ | $1 - \Omega_m$ | $-1.14^{+0.27}_{-0.35}$ | |
| E09 | X-ray | | $0.32 \pm 0.05$ | $1 - \Omega_m$ | $-1.1^{+0.7}_{-0.6}$ | |
| L06 | X-ray+SZ | | $0.40^{+0.28}_{-0.20}$ | $1 - \Omega_m$ | $-1$ | |
| **XSZ distances** | | | | | | |
| B06 | X-ray+SZ | | 0.3 | $1 - \Omega_m$ | $-1$ | $0.77^{+0.11}_{-0.09}$ |
| S04 | X-ray+SZ | | 0.3 | $1 - \Omega_m$ | $-1$ | $0.69 \pm 0.08$ |

From Allen et al. (2011)

# Current efforts and recent results

- Dark Energy Survey, Planck, South Pole Telescope, etc.
- Salvati et al. (2018) (cluster counts + SZ): Ωm = 0.32 ± 0.02, σ8 = 0.76 ± 0.03
- Ruppin et al. (2019) (SZ):

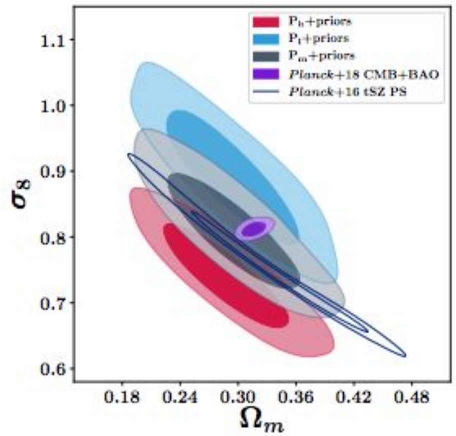


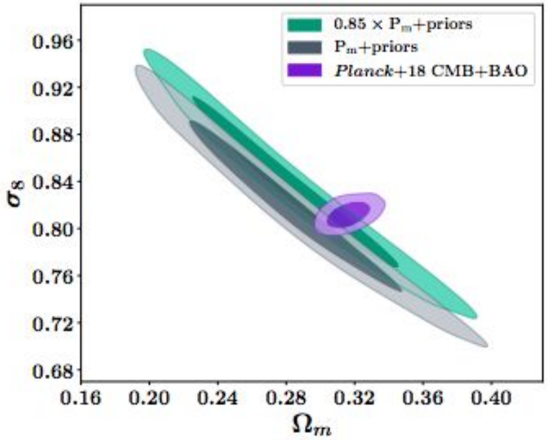

# Many factors can lead to systematic effects in galaxy cluster relations.

Probes related to galaxy dynamics typically assume simple dynamic models, with more complex dynamics lead to offsets in the various relations.

Many clusters deviate from hydrostatic equilibrium (10-20% in simulations), or have non-spherical geometry.

Clusters with cooling regions or strong cooling flows can cause significant scatter in L-T relation.

Assuming a larger scatter -> increased luminosity function -> lower normalization

One way to address intrinsic scatter is to convolve the function with the theoretical distribution of the scatter.

# SZ luminosity may be contaminated, biasing the X-ray luminosity.

Contamination is likely from small halos at the virial overdensity, which are expected to be present in large numbers and are currently unresolved.

Foreground and background sources may also be contaminants, and contribute to the same problems.

Diffuse gas in clusters is unlikely to be a significant factor, as the temperature and density for such gas is relatively low.

# Contamination introduces scatter into SZ relations

The scatter is worse in projection, and can be reduced if the redshifts are known.

Minimizing scatter is critical to use the SZ effect as a cosmological probe.

Figure from Borgani 2006

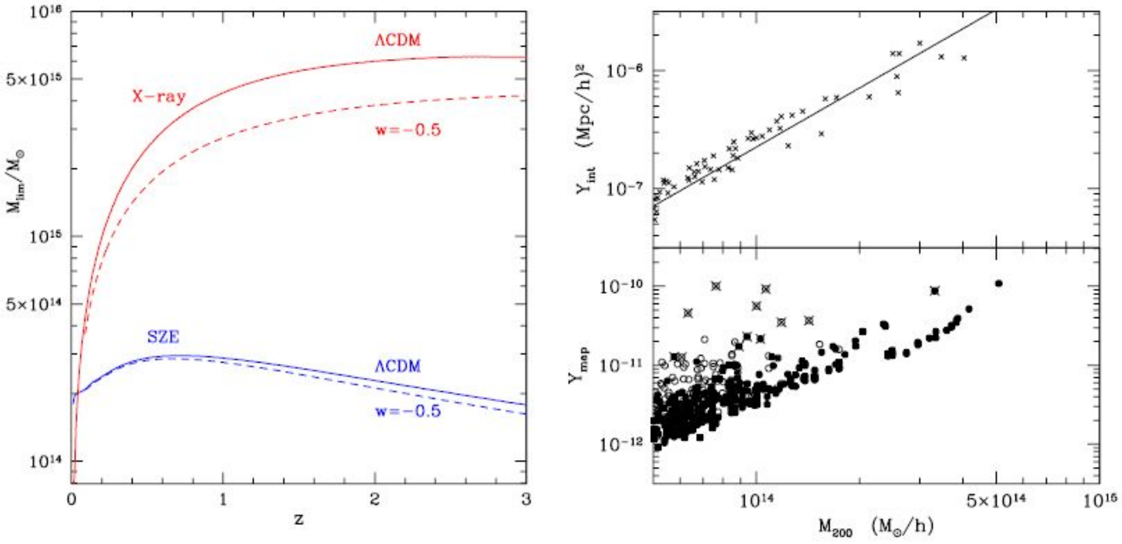


**Fig. 7.** Left panel: limiting cluster virial mass for detection in an X–ray and in a SZ survey (from [80]). Each pair of curves show the results for two $\Omega_m = 0.3$ cosmologies, having $w = -1$ and $w = -0.5$ for the DE equation of state. Right panel: the relation between the Comptonization parameter and $M_{200}$, from [168]. The upper panel shows the decrement contributed from the gas within $0.5R_{200}$. The lower panel indicates the signal from noise–free maps projected on the light cone.

# The selection function of galaxy clusters can introduce many systematics.

The selection function of a survey depends on its effective area as a function of flux.

Surveys will have different flux limits in different parts of the sky.

Translating across redshifts means that a survey can probe very different luminosity spaces as a function of cosmic time.

The selection function factors into every other relation, so not properly characterizing the selection function of your survey will introduce a multitude of systematic biases.

# In general, bias can be minimized by marginalizing over the probability distribution function of the desired parameters.

This increases the uncertainty of those parameters, but can account for systematic and statistical uncertainty.

This requires that the error be well-modelled.

The goodness of fit for such a marginalization is given by:

$$\chi^2(\mathbf{\Omega}) = \frac{\int \chi^2(\mathbf{\Omega}, \mathbf{W})\, P(\mathbf{W})\, d\mathbf{W}}{\int P(\mathbf{W})\, d\mathbf{W}}\,.$$

# Some systematic differences between simulations and observations can be calibrated out by using observational estimators.

$$\rho_{\rm gas}(r) = \frac{\rho_0}{[1 + (r/r_c)^2]^{3\beta/2}}$$

This estimator assumes hydrostatic equilibrium of a polytropic □-model.

It compresses the scatter due to intrinsic variation in thermal structure while adjusting the normalization.

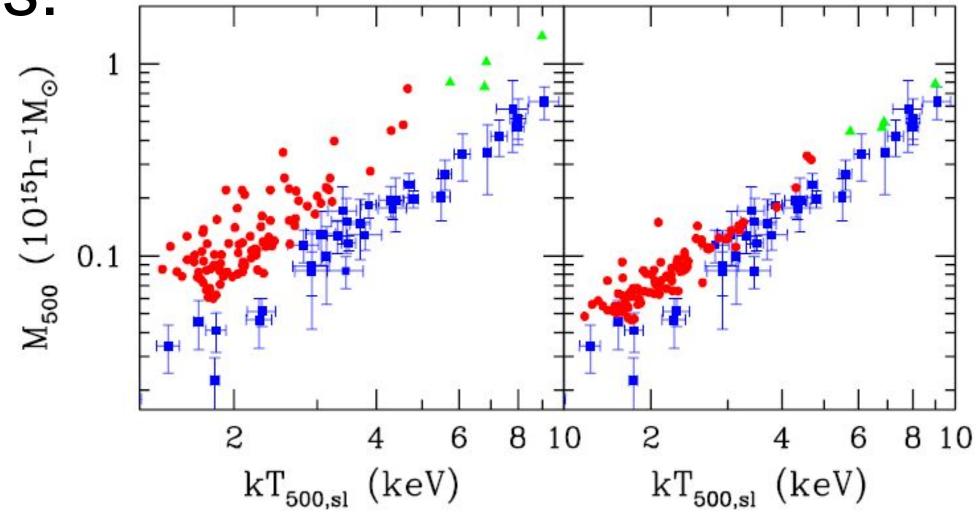


**Fig. 19.** The mass–temperature relation at $\bar{\rho}/\rho_{\rm cr} = 500$, in simulations (filled circles and triangles) and for the observational data (squares with errorbars, [62]). The left panel is for the true masses of simulated clusters; the right panel is for masses of simulated clusters estimated by adopting the same procedure applied by Finoguenov et al. to observational data (from [133]).

Figure from Borgani 2006

# References:


Allen S. W., Evrard A. E., & Mantz A. B., Annu. Rev. Astron. Astrophys. 2011. 49:409–70.

Borgani, Stefano. “Cosmology with Clusters of Galaxies.” arXiv:astro-ph/0605575v1, 2006.

Frieman J. A., Turner M. S., & Huterer D., Annu. Rev. Astron. Astrophys. 2008. 46:385–432.

Ruppin F., Mayet F., Macías-Pérez J. F., & Perotto L., 2019, arXiv:1905.05129.

Salvati L., Douspis M., & Aghanim N., 2018, A&A, 614, A13.